Supporting information for

Quantitative insights into regime-dependent aerosol pH variability in an ammonia-rich urban atmosphere from explainable machine learning

Jing Duan[1,†], Ting Wang[1,†], Ru-Jin Huang[1,2,3*], Jingye Ren[1], Haobin Zhong[4], Wei Xu[5], Chunshui Lin[1], Yanan Zhan[1,2], Huabin Huang[6], Yongjie Li[7]

[1]State Key Laboratory of Loess Science, Institute of Earth Environment, Chinese Academy of Sciences, Xi'an 710061, China

[2]Institute of Global Environmental Change, Xi'an Jiaotong University, Xi'an 710049, China

[3]University of Chinese Academy of Sciences, Beijing 100049, China

[4]School of Advanced Materials Engineering, Jiaxing Nanhu University, Jiaxing, 314001, China

[5]State Key Laboratory of Advanced Environmental Technology, Institute of Urban Environment, Chinese Academy of Sciences, Xiamen, China

[6]College of Environment and Public Health, Xiamen Huaxia University, Xiamen 361024, China

[7]Department of Civil and Environmental Engineering, Faculty of Science and Technology, University of Macau, Taipa, Macau SAR 999078, China

Correspondence to: Ru-Jin Huang (rujin.huang@ieecas.cn)

†Contributed equally to this study

Text S1. Sampling and instrumentation

The field campaign was carried out at an urban site located on the rooftop of a five-story building (~20 m above ground) at the National Center for Nanoscience in Beijing (39.99°N, 116.32°E). The site is situated near the 4th Ring Road and is influenced by mixed residential, commercial, and traffic emissions (Duan et al., 2020; Gu et al., 2020). Continuous measurements were performed from 21 December 2014 to 31 December 2015.

Non-refractory PM_1 (NR-PM_1) species, including organics (OA), sulfate (SO_4^{2-}), nitrate (NO_3^-), ammonium (NH_4^+), and chloride (Cl^-), were quantified using an Aerodyne quadrupole aerosol chemical speciation monitor (Q-ACSM) with a time resolution of ~30 min (Ng et al., 2011). Ambient aerosols were sampled through a 3/8 in. stainless-steel tube at a flow rate of ∼ 3 L min^{-1}, and the coarse particles were removed by an University Research Glassware (URG) cyclone (model: URG2000-30ED) with a 2.5 μm cut in front of the sampling inlet. Before entering the ACSM, particles were dried using a Nafion dryer (MD110-48S; Perma Pure, Inc., Lakewood, NJ, USA). The dried submicron aerosol was then subsampled into the ACSM at 85 cc min^{-1}, controlled by a 100 μm critical orifice. Within the ACSM, particles were focused into a narrow beam by an aerodynamic lens and vaporized on a heated surface (~600 °C). The resulting vapor was ionized with electron impact and chemically characterized with a quadrupole mass spectrometer. Instrument calibration was carried out using monodisperse 300 nm ammonium nitrate particles generated by an atomizer (Model 9302, TSI Inc., Shoreview, MN, USA) and size-selected by a differential mobility analyzer (DMA; TSI Model 3080) to determine the response factor (RF) and ionization efficiency (IE) (Ng et al., 2011).

Ambient ammonia (NH_3) concentrations were measured using a Picarro G2103 analyzer (Picarro Inc., USA), which employs wavelength-scanning optical cavity ring down spectroscopy (WS-CRDS). This technique is capable of measuring NH_3 with a parts-per-trillion (ppt) sensitivity based on a sophisticated time-based measurement system (Maasikmets et al., 2015). The G2103 is equipped with high-precision temperature and pressure control systems to ensure the highest accuracy and lowest drift. In addition, the G2103 offers a large dynamic range, providing linear response into the parts-per-million (ppm) range without dilution, concentration and sample preparation.

Meteorological parameters, including temperature and relative humidity (RH), were simultaneously recorded by an automatic weather station (MAWS201, Vaisala, Vantaa, Finland).

Text S2. Calculation of excess NHx

Excess NHx in this study represents the portion of total NHx (gas-phase NH_3 plus particle-phase NH_4^+) that remains after neutralizing the major inorganic acidic species (SO_4^{2-}, NO_3^-, and Cl^-) in the aerosol (i.e., the required NHx) (Liu et al., 2017).

Thus, excess NHx is defined as:

Excess NHx = Total NHx- Requid NHx

Where

$$\text{Total NHx} = 17 \times \left(\frac{[NH_3]}{17} + \frac{[NH_4^+]}{18}\right) \quad (1)$$

$$\text{Required NHx} = 17 \times \left(\frac{[SO_4^{2-}]}{48} + \frac{[NO_3^-]}{62} + \frac{[Cl^-]}{35.5}\right) \quad (2)$$

$[NH_3]$, $[NH_4^+]$, $[SO_4^{2-}]$, $[NO_3^-]$, and $[Cl^-]$ are the measured mass concentrations (μg m^{-3}). A positive excess NHx (μg m^{-3}) indicates ammonia-rich conditions, whereas a negative value denotes ammonia-poor conditions (Song et al., 2018).

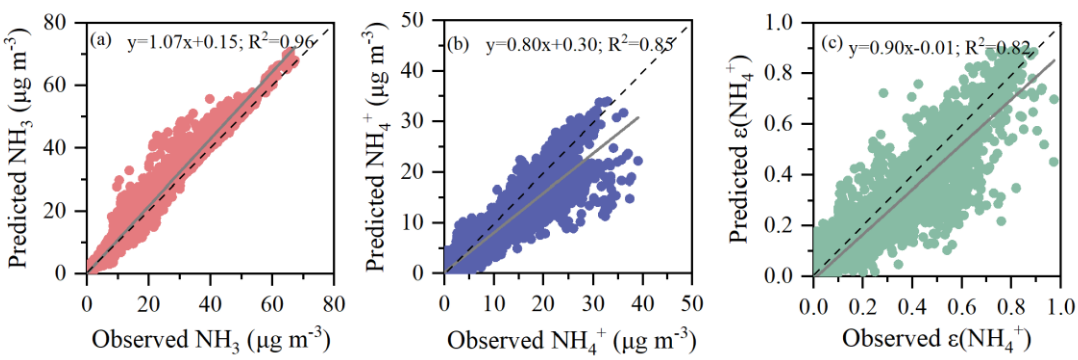

Figure S1. Comparisons between predicted and observed values for NH_3 (a), NH_4^+ (b), and $\varepsilon(NH_4^+)$ (c). $\varepsilon(NH_4^+)$ is calculated as the molar ratio of $NH_4^+/(NH_4^++NH_3)$.

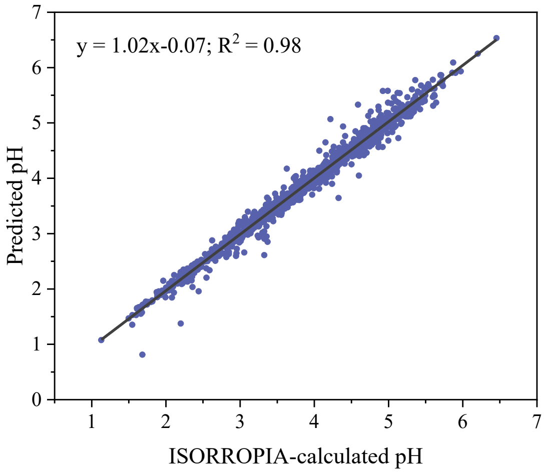

Figure S2. Correlation between aerosol pH predicted by XGBoost model and pH calculated using ISORRPOIA II.

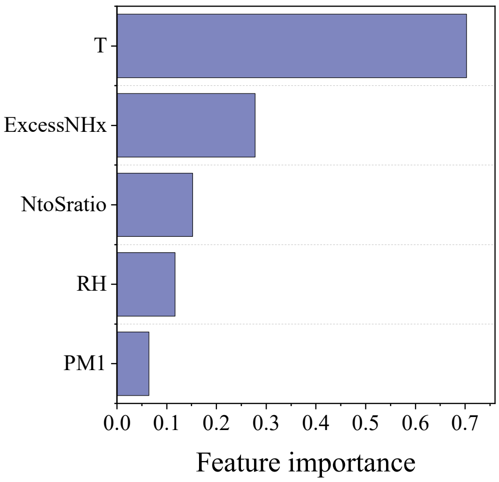

Figure S3. Feature importance for aerosol pH over the entire sampling period based on mean absolute SHAP values, showing the relative influence of each predictor on the model output.

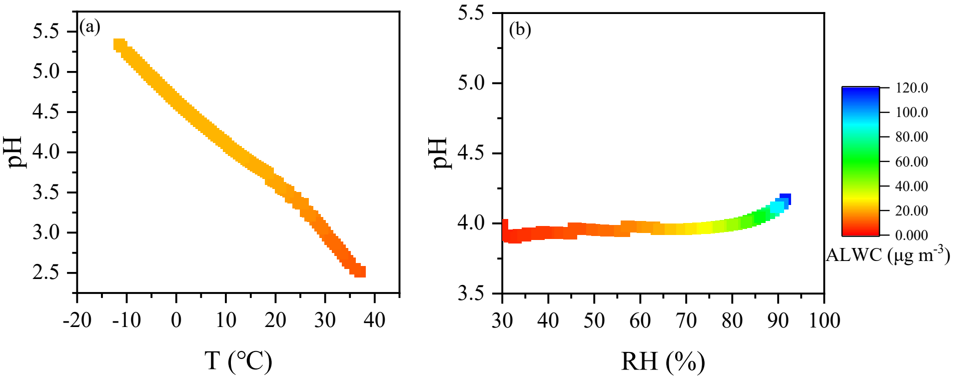

Figure S4. ISORROPIA II sensitivity tests of pH to temperature (a) and RH (b). In this analysis, the real-time measured values of the tested variable, while the average values of the other species were applied as the input into ISORROPIA II.

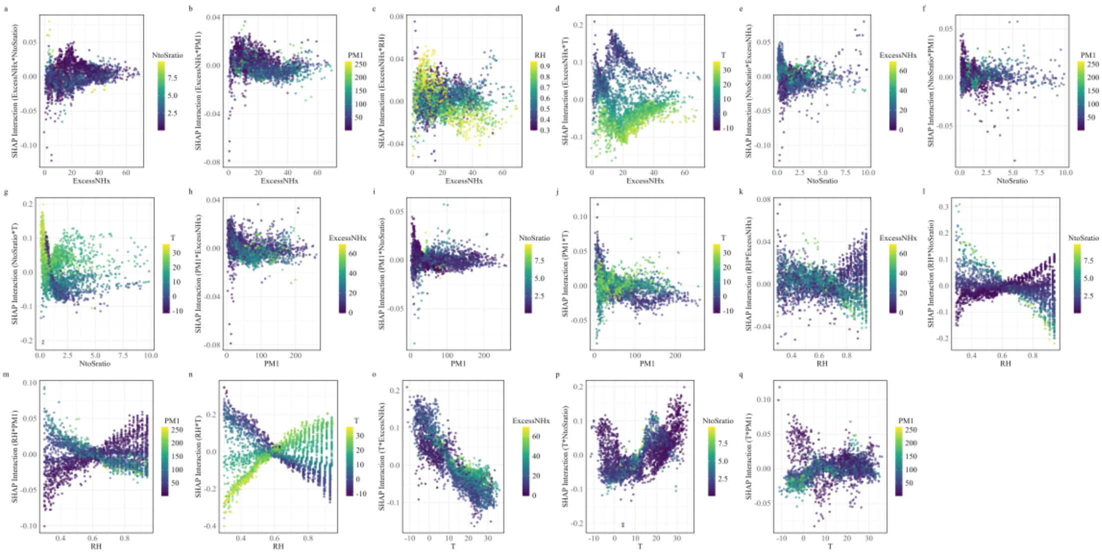

Figure S5. Summary plots of the SHAP interaction matrix values for pH among each pair of variables, excluding RH vs T, RH vs N/S ratio, and RH vs PM_1 mass, which are discussed in detail in the manuscript.

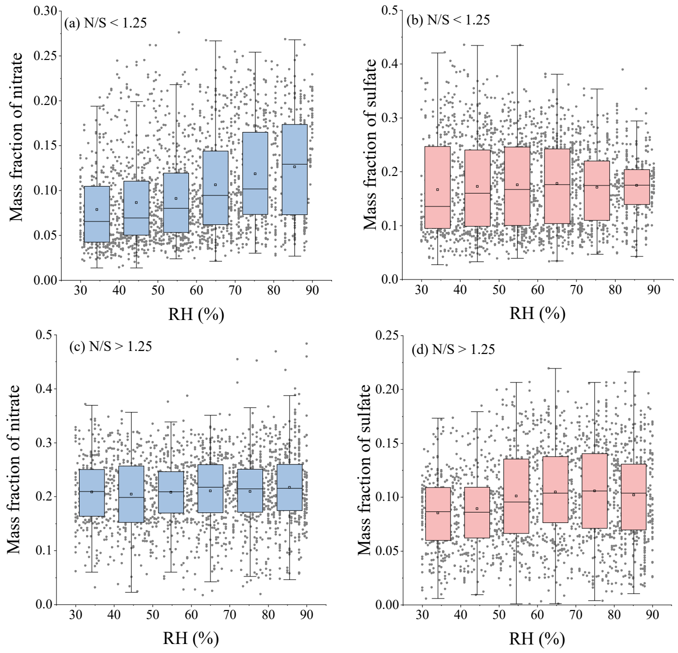

Figure S6. The variations in nitrate and sulfate mass fractions with RH under sulfate-dominant conditions (N/S < 1.25) (a, b) and nitrate-dominant conditions (N/S > 1.25) (c, d), respectively. The whiskers, floating boxes, lines, and squares inside the boxes denote the 10th and 90th distributions, 25th-75th ranges, median values, and mean values, respectively.

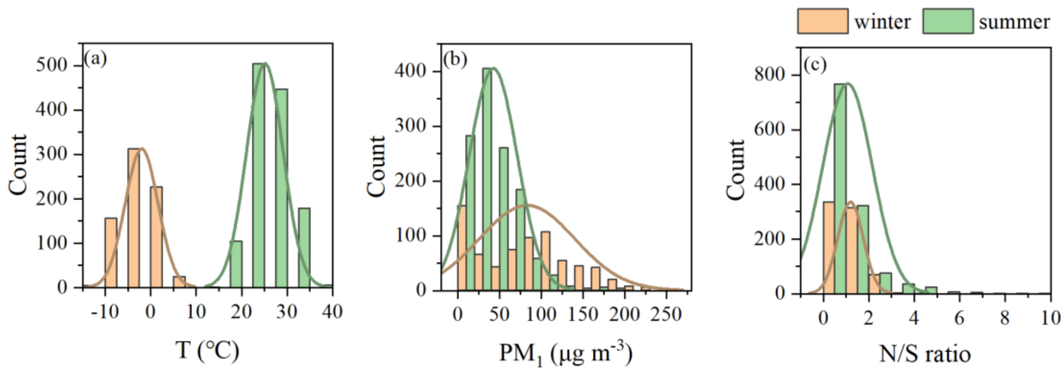

Figure S7. The distribution of temperature (a), PM_1 mass loading (b), and nitrate-to-sulfate (N/S) mass ratio (c) between summer and winter periods.

Reference

Duan, J., Huang, R.-J., Li, Y., Chen, Q., Zheng, Y., Chen, Y., Lin, C., Ni, H., Wang, M., Ovadnevaite, J., Ceburnis, D., Chen, C., Worsnop, D. R., Hoffmann, T., O'Dowd, C., and

Cao, J.: Summertime and wintertime atmospheric processes of secondary aerosol in Beijing, Atmos. Chem. Phys., 20, 3793-3807, 10.5194/acp-20-3793-2020, 2020.

Gu, Y., Huang, R. J., Li, Y., Duan, J., Chen, Q., Hu, W., Zheng, Y., Lin, C., Ni, H., Dai, W., Cao, J., Liu, Q., Chen, Y., Chen, C., Ovadnevaite, J., Ceburnis, D., and O'Dowd, C.: Chemical nature and sources of fine particles in urban Beijing: Seasonality and formation mechanisms, Environ. Int., 140, 105732, 10.1016/j.envint.2020.105732, 2020.

Liu, M., Song, Y., Zhou, T., Xu, Z., Yan, C., Zheng, M., Wu, Z., Hu, M., Wu, Y., and Zhu, T.: Fine particle pH during severe haze episodes in northern China, Geophys. Res. Lett., 44, 5213-5221, 10.1002/2017gl073210, 2017.

Maasikmets, M., Teinemaa, E., Kaasik, A., and Kimmel, V.: Measurement and analysis of ammonia, hydrogen sulphide and odour emissions from the cattle farming in Estonia, Biosyst. Eng., 139, 48-59, 10.1016/j.biosystemseng.2015.08.002, 2015.

Ng, N. L., Herndon, S. C., Trimborn, A., Canagaratna, M. R., Croteau, P. L., Onasch, T. B., Sueper, D., Worsnop, D. R., Zhang, Q., Sun, Y. L., and Jayne, J. T.: An Aerosol Chemical Speciation Monitor (ACSM) for Routine Monitoring of the Composition and Mass Concentrations of Ambient Aerosol, Aerosol. Sci. Tech., 45, 780-794, 10.1080/02786826.2011.560211, 2011.

Song, S., Gao, M., Xu, W., Shao, J., Shi, G., Wang, S., Wang, Y., Sun, Y., and McElroy, M. B.: Fine-particle pH for Beijing winter haze as inferred from different thermodynamic equilibrium models, Atmos. Chem. Phys., 18, 7423-7438, 10.5194/acp-18-7423-2018, 2018.